

RECONFIGURABLE POINTING CONTROL FOR HIGH RESOLUTION SPACE SPECTROSCOPY

David S. Bayard and Tooraj Kia
 Jet Propulsion Laboratory
 California Institute of Technology
 4800 Oak Grove Drive
 Pasadena, CA 91109

Jeffrey Van Cleve
 Department of Astronomy
 Cornell University
 Ithaca, NY 14853

Abstract

In this paper, a pointing control performance criteria is established to support high resolution space spectroscopy. Results indicate that these pointing requirements are very stringent, and would typically be difficult to meet using standard **3-axis** spacecraft control. To resolve this difficulty, it is shown that performance can be significantly improved using a **reconfigurable** control architecture that switches among a small bank of **detuned Kalman** filters. The effectiveness of the control reconfiguration approach is demonstrated by example on the Space **Infra-Red** Telescope Facility (**SIRTF**) pointing system, in support of the Infrared Spectrograph (IRS) payload.

1 Introduction

Spectroscopy measurements are important for many types of scientific observations, and as a result are used in a wide variety of spacecraft payloads. For example, NASA's Space **Infra-Red** Telescope Facility (**SIRTF**), is expected to carry the **InfraRed** Spectrograph (IRS) payload to obtain various high-resolution spectrographs of interstellar, matter, planetary nebula and galactic nuclei.

High resolution spectroscopy depends on the accurate determination of the ratios of measured spectral lines. This requires that the flux obtained during measurement is not significantly degraded (i.e., offset) by motion of the image spot in the entrance slit during the exposure. Because of properties of the slit geometry and the imaging optics, the flux offset varies as a complicated function of both the pointing hiss and jitter [4][5][6].

In Section 2, a pointing control performance criteria is established to support high resolution space spectroscopy. In **contrast** to the case of imaging instruments which degrade (i.e., blur) primarily as a simple function of the jitter, the flux **offset** is shown to vary as a nontrivial function of both the pointing hiss and jitter [1] [4] [5] [6]. Due to this dependence on both bias and jitter, it is shown that typical pointing requirements needed to support high-resolution spectroscopy are quite stringent, and would typically be **difficult** to meet using standard **3-axis** spacecraft control.

To resolve this difficulty, it is shown in Section 3 that performance can be significantly improved using a **reconfigurable** control architecture that switches among a small bank of **detuned Kalman** filters. The effectiveness of the control reconfiguration approach is demonstrated by example on the **SIRTF** pointing system, in support of the IRS payload. Conclusions are postponed until Section 4.

2 Pointing Requirements

2.1 Signal Diagram

A detailed signal diagram representing the spectroscopy requirements is shown in Figure 1. The quantity $w_o(\tau)$ represents the pointing process, which is assumed to be a second-order stationary **Gaussian** random process with mean w_b and variance σ_a^2 . In pointing control language, w_b is defined as the **bias** and σ_a is the long-term jitter, i.e., the **RMS** jitter associated with windows of infinite duration.

The pointing process $w_o(\tau)$ is expressed in units of **arcseconds**, and is defined with respect to the slit center. For example, if $w_o = 0$ the image spot will be directly at the slit center. The coefficient A_2 of the square law has units of $(\text{arcsec})^{-2}$ so that the quantities ξ and x are dimensionless. The coefficient A_2 is determined

by fitting curves depicting fractional flux offset versus position, **and** is in general a function of slit geometry, wavelength, and the optical design [4]. Only motion along the slit width (i.e., the dispersion direction) is considered in the analysis since performance is relatively insensitive to motion along the **slit** length. As a result, **all** expressions will be in terms of single axis requirements resolved along the dispersion direction.

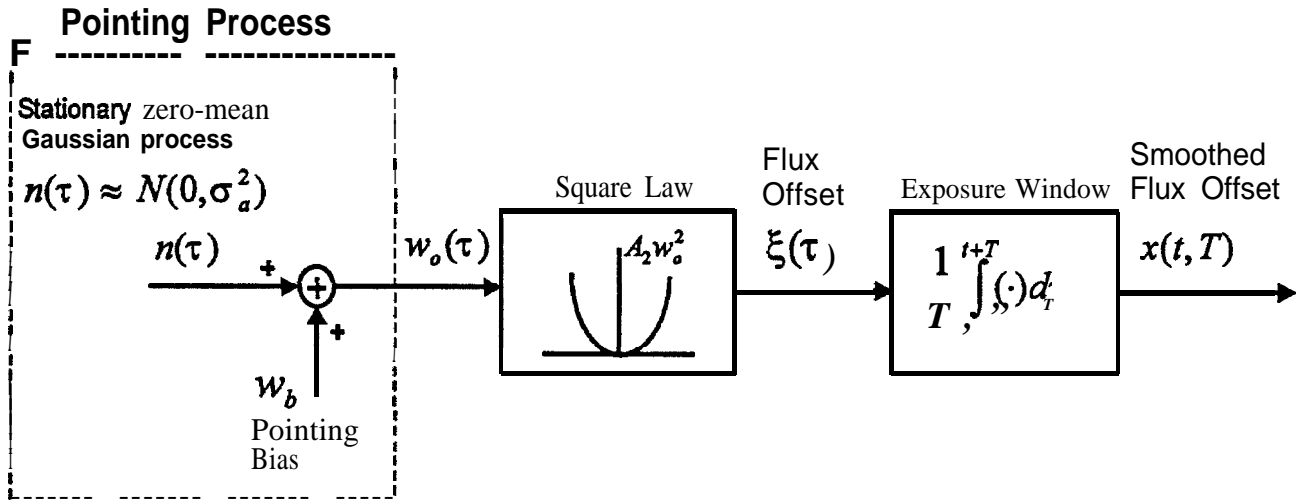


Figure 1: Signal diagram for spectroscopy pointing requirements

2.2 Statistical Analysis

The pointing control objective is to keep the image spot in the center of the slit **by** keeping the smoothed flux offset x small. Specifically, for accurate **measured** line ratios, it is desired that the probability of x exceeding a specified threshold d be **less** than a specified probability α . Equivalently,

$$P_x(x \geq d) \leq \alpha \quad (1)$$

where $P_x(\cdot)$ is the probability distribution of $x(t, T)$ in Figure 1. Since $x(t, T)$ is a stationary process in time, the probability P_x will not depend on t , but will in general be a function of the exposure time 'T'.

Let $x_{1-\alpha}$ be the $(1 - \alpha)\%$ percentile of the random variable x defined as follows,

$$P_x(x \geq x_{1-\alpha}) = \alpha \quad (2)$$

Then the pointing condition (1) can be equivalently written as,

$$x_{1-\alpha} \leq d \quad (3)$$

For infinite-time exposures (i.e., $T \rightarrow \infty$), the percentile $x_{1-\alpha}$ can be evaluated analytically as [1],

$$x_{1-\alpha} = A_2(\sigma_a^2 + w_b^2) \quad \text{valid for } T \rightarrow \infty \quad (4)$$

Unfortunately, for exposures of finite duration T , expression (4) is not valid, and the percentile $x_{1-\alpha}$ is much more difficult to evaluate. Hence, it will be replaced by an **overbound** $\tilde{x}_{1-\alpha}$, which can be used to enforce (3) **as** follows,

$$x_{1-\alpha} \leq \tilde{x}_{1-\alpha} \leq d \quad (5)$$

In [1], using **Bienayme's** inequality (Papoulis [2] pp. 115), such an **overbound** is obtained of the form,

$$\tilde{x}_{1-\alpha} = \frac{A_2}{\sqrt{\alpha}} \cdot [3(\sigma_a^2 + w_b^2)^2 - 2w_b^4]^{\frac{1}{2}} \quad \text{valid for any } T \geq 0 \quad (6)$$

Using (6) in (5) and rearranging gives the pointing requirement,

$$[3(\sigma_a^2 + w_b^2)^2 - 2w_b^4]^{\frac{1}{2}} \leq \sqrt{\alpha} \cdot \frac{d}{A_2} \quad (7)$$

It is emphasized that (7) is very different from requirements for imaging instruments which avoid **smearing** by **constraining** the allowable **RMS** jitter over a window of specified duration (cf., [3]). In contrast, requirement (7) **simultaneously** constrains both the pointing hiss and jitter.

2.3 Three-Axis Control

As a realistic example, consider the values $\alpha = .05$ (for 95% confidence), $A_2 = .13$, and $d = .07$ (i.e., from the SIRTIF IRS [4]). Substituting these values into (7), assuming equal contributions from bias and jitter gives,

$$\sigma_a = |\omega_b| \leq .195 \text{ arcseconds} \quad (8)$$

While it may be possible to meet the jitter requirement by taking advantage of optimal filtering and a good gyro/tracker combination, these requirements are quite stringent from the bias point of view. For example, a bias error of .2 arcseconds is by itself smaller than the accuracy of most available star trackers, and in addition there will be many other factors contributing to the overall pointing bias.

3 Reconfigurable Control

3.1 Architecture

It was seen that pointing requirements for high resolution spectroscopy are difficult to meet using standard 3-axis spacecraft control. An alternative approach based on a reconfigurable controller is proposed in this section. The basic idea is to place the image spot into the slit using a precision incremental maneuver on gyros, which avoids the bias error associated with the star tracker.

The proposed reconfigurable control architecture is shown in Figure 2. Here, KF1 and KF2 are Kalman filters which have been detuned to have time constants τ_1 and τ_2 , respectively. KF1 and KF2 are both driven by the measured position quaternion q_m and measured 3-axis rate ω_m , while KFg is the optimal Kalman filter designed only with a rate measurement input. In this scheme, KF1 and KF2 are free running filters, while KFg is initialized by KF1 at time $t = 0$.

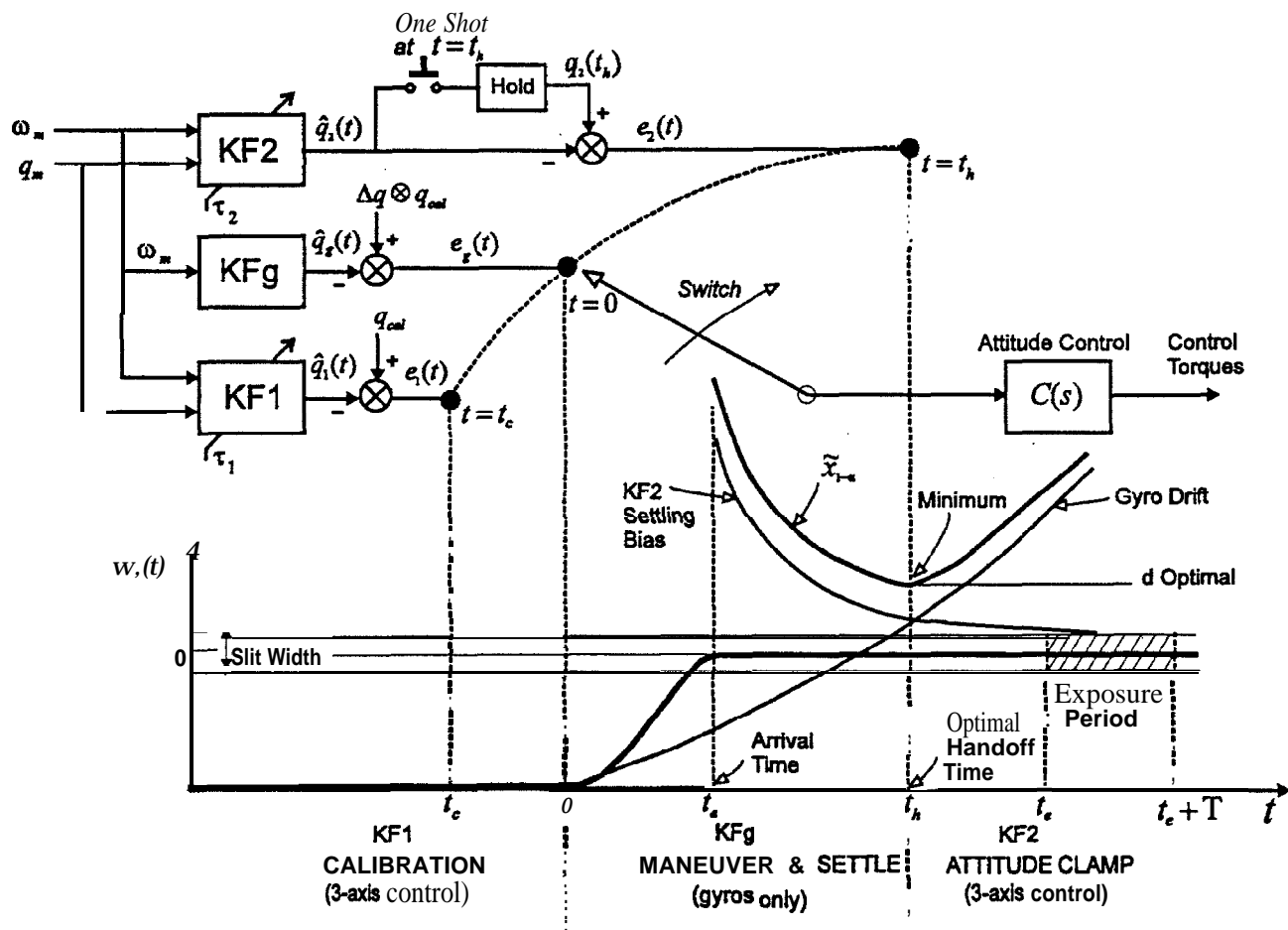


Figure 2: Reconfigurable control architecture for high-resolution spectroscopy

3.2 Handoff Description

As shown in Figure 2, the error signal which drives the attitude controller is taken from KF1 at time $t = t_c$, and is switched to KFg at time $t = 0$, and is switched to KF2 at time $t = t_h$. It is assumed that the telescope and star tracker are in different frames, and that the body frame is the star tracker frame. Details of the particular handoff sequence are given below,

1. Point telescope to calibration source at attitude q_{cal} by nulling control error $e_1(t)$ associated with KF1.
2. Calibrate frame misalignment between tracker and telescope using calibration source (as imaged on a detector in the telescope frame) during time interval $t_c \leq t \leq 0$ while holding attitude on KF1.
3. Calculate incremental offset Δq in body frame needed to put a target source with known J2000 coordinates into center of spectroscopy slit.
4. At time $t = 0$, command the attitude $\Delta q \otimes q_{cal}$ [where \otimes denotes standard quaternion multiplication], and null control error $e_g(t)$ associated with KFg to implement maneuver.
5. Target arrives at slit at time $t = t_a > 0$.
6. At $t = t_h \geq t_a$ sample the "one-shot" to clamp attitude estimate associated with KF2, and null the control error $e_2(t)$.
7. Hold attitude by nulling $e_2(t)$ until spectroscopy exposure of duration T is completed.

It is emphasized that the attitude estimate from KF2 is clamped at time t_h to generate the control error $e_2(t)$ to be nulled. No effort is made to reconcile the estimate from KF2 with the estimate from KFg, since this would typically cause a large jump in the combined state estimate at time t_h (on the order of the tracker bias) which could kick the image spot out of the slit. In fact, this is the reason that standard 3-axis control fails, and is avoided in the reconfigurable control concept.

3.3 Covariance Analysis

A single axis covariance analysis is given below, to characterize behavior along the slit dispersion direction.

Given desired time constant τ , the Kalman filter gains k_1 and k_2 (associated with a two-state observer of single-axis position and gyro hiss) are detuned as follows. Let $\omega_{kf} \triangleq \left(\frac{q_2}{r}\right)^{\frac{1}{2}}$.

- If $\frac{1}{\tau} \leq \omega_{kf}$ then use complex roots: set $k_1 = \frac{2}{\tau}$ and $k_2 = \omega_{kf}^2$.
- If $\frac{1}{\tau} > \omega_{kf}$ then use repeated real roots: set $k_1 = \frac{2}{\tau}$ and $k_2 = \frac{1}{\tau^2}$.

The steady-state covariances associated with the detuned Kalman filters can be calculated as,

$$p_{11} = \frac{r(k_2^2 + k_1^2 k_2) + q_1 k_2 + q_2}{2k_1 k_2}, \quad p_{12} = \frac{r k_2^2 + q_2}{2k_2} \quad (9)$$

$$p_{22} = \frac{r(k_2^3 + k_1^2 k_2^2) + q_1 k_2^2 + q_2(k_2 + k_1^2)}{2k_1 k_2} \quad (10)$$

$$P \triangleq E[ee^T] = \begin{bmatrix} p_{11} & p_{12} \\ p_{12} & p_{22} \end{bmatrix} \quad (11)$$

where $e = [\delta\theta, \delta b]^T$, $\delta\theta = \theta - \hat{\theta}$ is the error in the angular position estimate, $\delta b = b - \hat{b}$ is the error in the gyro bias estimate, and,

- q_1 - Gyro Angle Random Walk Covariance (rad^2/sec)
- q_2 - Gyro Bias Instability Covariance (rad^2/sec^3)
- r - Equivalent CT Tracker noise covariance (rad^2)
 $r = \Delta \sigma_{nea}^2 / N$
- Δ - Tracker Sampling Period (see)
- σ_{nea} - hacker NEA (per star, 1-sigma)
- N - Number of stars on Tracker FOV

The pointing jitter after handoff can be calculated as,

$$\sigma_a^2 = \beta^2 \cdot p_{11}(\tau_2) \quad (12)$$

where $p_{11}(\tau_2)$ is the position estimation error covariance of KF2, and $\beta = 206265$ is a scale factor to convert radians to arcseconds. The quantity σ_a^2 will generally increase as KF2 is detuned further (i.e., as τ_2 is decreased).

The total pointing bias after handoff can be calculated as,

$$w_b^2 = \sigma_g^2(t) + \sigma_p^2 + \sigma_s^2 + \sigma_m^2 + \sigma_c^2 + \sigma_a^2 + \sigma_{KF2}^2(t) \quad (13)$$

where,

- σ_g - Gyro Drift
- σ_p - Body-to-Telescope Frame Misalignment error
- σ_s - Gyro Scale Factor Error
- σ_m - Gyro Frame Misalignment Error
- σ_c - Steady-State Control Bias Error (after handoff)
- σ_{KF2} - Bias from Kalman Filter KF2 settling
- w_{iru} - Tracker bias change (over maneuver)

The jitter term σ_a^2 reappears in the bias expression (13) because at time $t = t_h$ one is clamping onto the random (rather than deterministic) process associated with KF2. The time-varying terms $\sigma_g^2(t)$ and $\sigma_{KF2}^2(t)$ dominate the expression for the bias (13) and deserve closer attention. The gyro drift is given by,

$$\sigma_g^2(t) = \beta^2 \cdot \left[\frac{q_2}{3} t^3 + p_{22}(\tau_1) t^2 + (2p_{12}(\tau_1) + q_1) t + p_{11}(\tau_1) \right] \quad (14)$$

where $p_{ij}(\tau_1)$ are steady-state covariances from the detuned filter KF1. As shown in Figure 2 the gyro drift increases monotonically with time after $t = 0$. The settling bias of KF2 is given by,

$$\sigma_{KF2}(t) = w_{iru} e^{-(t-t_a)/\tau_2} \quad (15)$$

where τ_2 is the time constant (by design) associated with KF2. This is the error associated with clamping onto the filter KF2 before it has completely settled, As shown in Figure 2 the settling bias decreases monotonically with time after $t = t_a$.

3.4 Application to SIRTF IRS

The reconfigurable control concept is applied to the SIRTF telescope in support of the IRS payload. Parameters associated with a candidate SIRTF pointing control design are given as $q_1 = 3.3846e - 15 \text{ rad}^2/\text{sec}$, $q_2 = 7.3451e - 21 \text{ rad}^2/\text{sec}^3$, $r = 1.0581e - 12 \text{ rad}^2$, $\sigma_p = \sigma_s = \sigma_m = \sigma_c = .1 \text{ arcsec}$, $w_{iru} = .4 \text{ arcsec}$, where a 30 arcmin maneuver has been assumed, Parameters relevant to the IRS payload are given as [4] $A_2 = .13 (\text{arcsec})^{-2}$, $d = .07$, $\alpha = .05$.

Equation (12) for σ_a^2 and (13) for w_b^2 are substituted into (6) to give the quantity $\tilde{x}_{.95}$ for $t \geq t_a$, which is plotted in Figure 3 for different values of $\tau_1 = 10, 20, 30$ and $\tau_2 = 10, 20, 30$. If the handoff is timed to catch the minimum of each curve, it is seen that the desired value of $d = .07$ can be satisfied with any one of several possible designs. For example one reasonable design would be $\tau_1 = 20, \tau_2 = 20$ which requires optimal handoff at $t = t_a + 30$ seconds, and achieves a performance better than $d = .06$. Without reconfiguration, a 3-axis controller for the same example would perform no better than $d = .12$, and would have additional drift terms which have not been analyzed here.

4 Conclusions

A pointing control performance criteria has been established in support of high resolution space spectroscopy. The requirement, given by (7), simultaneously constrains both the pointing bias and jitter to ensure that the flux offset is small in the sense that it is less than a specified fractional error d with at least $(1 - \alpha) \times 100\%$ percent confidence. Calculations indicated that these pointing requirements would be difficult to meet using standard 3-axis spacecraft control primarily due to a tight pointing hiss requirement.

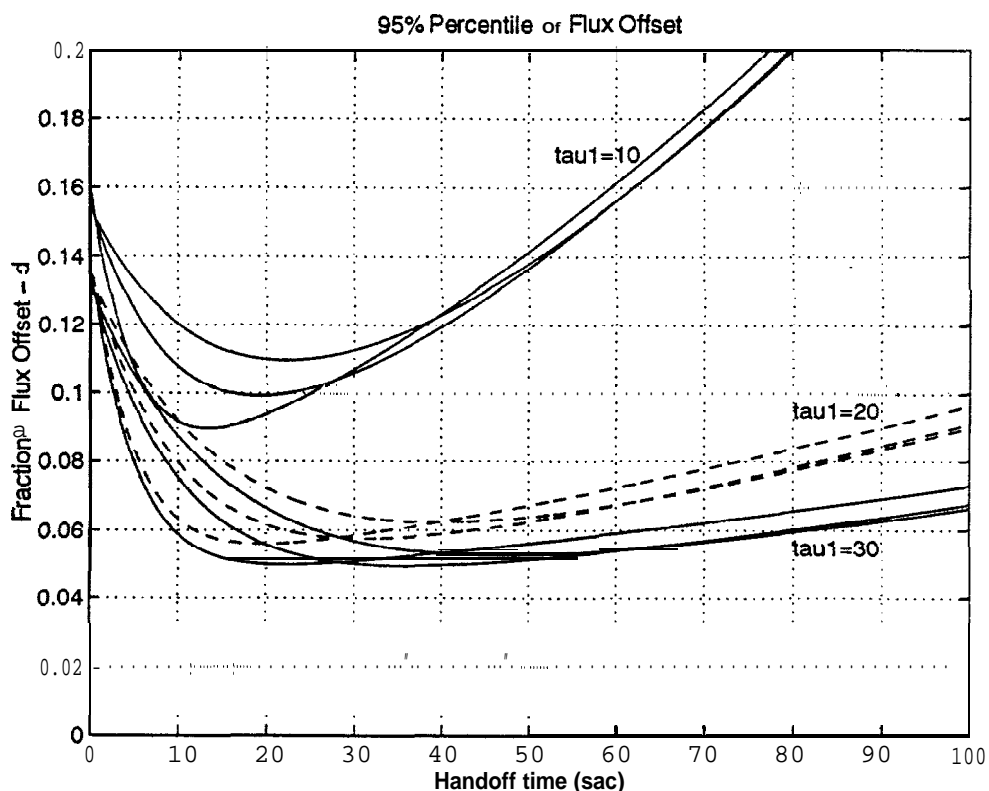


Figure 3: Optimal Handoff Timing and Performance

In order to satisfy the performance requirement, a **reconfigurable** control concept **was** proposed which avoids to a large extent the contribution of the bias error from the star tracker. The effectiveness of the control reconfiguration approach was demonstrated on the **SIRTF** pointing system in support of the IRS payload. Results indicate that by proper choice of filter **detuning** and optimized handoff timing, **the flux** offset can be held (with ,95 probability) to within $d = .06$ of the ideal flux. This contrasts with $d = .12$ for the **3-axis** control design, and results in significantly improved high-resolution science capability.

Acknowledgements

The authors would like to thank Fernando **Tolivar** of **JPL** for several technical discussions. This research was performed at the Jet Propulsion Laboratory, California Institute of Technology, under contract with the National Aeronautics and Space Administration,

References

- [1] D.S. Bayard and T, Kia, "IRS Pointing Requirements for **SIRTF** Under 3-Axis Control," **JPL** Internal Document, Engineering Memorandum **EM-3454-97-008**, November 13, 1996.
- [2] A. Papoulis, *Probability, Random Variables and Stochastic Processes.*, Second Edition, McGraw Hill, New York, 1984.
- [3] S.W. Sirlin, A.M. San Martin, "A New Definition of Pointing Stability," **JPL** Internal Document, Engineering Memorandum **EM 343-1189**, March 6, 1990.
- [4] J. Van Cleve, "SIRTF Pointing Requirements Derived from **Slit Transmission** in the Diffraction Limit," Report, Dept. of Astronomy, Cornell University, Ithaca NY, May 14, 1991.
- [5] J. Van Cleve, "Jitter-Drift Pointing Requirements for **SIRTF-IRS**," Report, Dept. of Astronomy, Cornell University, Ithaca NY, July 10, 1995.
- [6] J. Van Cleve, "Accuracy and Reconstruction Models," Report, Dept. of Astronomy, Cornell University, Ithaca NY, September 10, 1996.